Paper: ASAT-16-110-PP

16th International Conference on
AEROSPACE SCIENCES & AVIATION TECHNOLOGY,
ASAT - 16 – May 26 - 28, 2015, E-Mail: asat@mtc.edu.eg
Military Technical College, Kobry Elkobbah, Cairo, Egypt
Tel : +(202) 24025292 – 24036138, Fax: +(202) 22621908

METALIZED FUEL HYBRID ROCKET MOTOR PARAMETRIC STUDY

Ah. El-S. Makled*

ABSTRACT

The objective of this paper is to study theoretically and experimentally the effects of different design parameters on hybrid rocket motor (HRM). HRM propellant constituents are Polyethylene (PE) with Al powder additive as solid fuel and gaseous oxygen (GO2) as oxidizer. The study has been extended to cover the important phenomena such as throttling operation, exhaust flame (plume) and the results are given in the form of tables and graphs for quick and easy analysis.

The effect of several design parameters on system performance under consideration was investigated. These parameters are the fuel grain port-diameter, oxidizer mass flow rate and Al powder additives.

Focusing on the use of Al powder weight percentage additives to formulate, improve the regression rate and performance as compared to conventional hybrid motor (pure PE+GO_2). Regression rate of hybrid fuel grain was enhanced by addition of Al powder. Adding up to 7.5% gives the best performance as regression rate increases by 90% and chamber pressure increases by 40% compared to basic configuration (0% Al).

The present work is to aid the designer to carry out optimization of HRM to increase the combustion efficiency and to better control the operating parameters.

KEY WORDS

Hybrid Rocket Motor, Regression rate, metal powder additive.

1: INTRODUCTION

Sergei P. Korolev and Mikhail K. Tikhonravov reported the first recorded effort, as a forerunner to the hybrid rocket, within the scope of the Russian GIRD. A flight was made of the GIRD-09 on 17 August 1933. It was approximately 17.5 cm in diameter by 2.4 m long, had a thrust of 500 N for 15 s and attained an altitude of 1500 m [1,2].

Over a 40 years span from 1970 to 2011, the technology of hybrid propulsion motors (HPM) advanced rapidly by French [3], German [4,5], Swedish [6], Israel [7,8,9], India [10,11], United States [12,13,14] and recently England activities [15,16,17].

The four types of chemical propulsion systems; including liquid, solid, hybrid-propellant propulsion systems and ramjet, they are shown in **Figure (1)**.

The third type is hybrid propulsion, which employs propellant ingredients separated both physically and by phase. Solid fuel ramjets are similar to hybrids, but the oxidizer is not stored onboard. **Table (1)** gives the relative performance comparison of the abovementioned chemical rocket systems.

Until now, regression rates of conventional solid fuels have typically been an order of magnitude lower than approximately 1/3 time of that of solid propellants. Hence, a relatively large fuel-surface area is required to produce a desired thrust level [18].

* Ph.D., Egyptian Armed forces

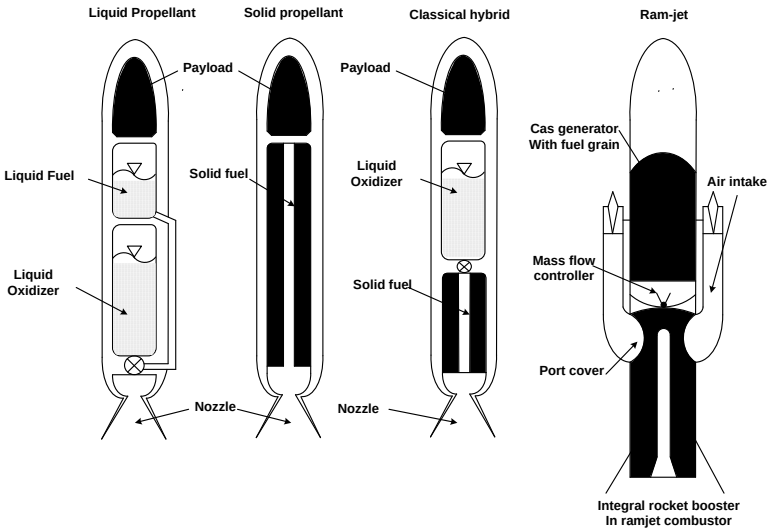

Fig. (1) Types of Chemical Propulsions Systems

Table (1) Chemical Propulsion Systems Characteristics and Performances [18,19]

Properties	Liquid Engine	Solid Motor	Hybrid Engine	Ram-Jet Engine
I_{sp} (s)	140-480	260-300	290-380	1200
Propellant density (kg/m3)	850-1150	About 1900	About 900	1200
Regression rate range	----------	High & wide range	Limited (1/3 SPRM)	Between solid& hybrid
Safety	Approximately safe	Easy to explode	More safe	SRJ (very safe) LRJ (safe)
Simplicity	Bi-prop. complicated	Very simple	Between solid & liquid	Between solid& hybrid
Reliability	Acceptable	Higher	High	High
Thrust control	Excellent	Difficult to apply	Fair	SRJ (fair) LRJ(excellent)
Nozzle erosion	Very low	Low	High	Low
On-off operation	Excellent	None	Fair	SRJ (difficult) LRJ (fair)
Sliver	< 1%	<< 2%	About 6%	< 1%
Comb. efficiency	About 99%	About 97%	About 90%	About 90%
Temp. independency	Acceptable	Highly sensitive	Very low sensitive	Between solid& hybrid
Grain cracks effect	None	High	Low	Between solid& hybrid
Stable combustion	more stable	Related to grain shape	Acceptable	Acceptable

Due to the mechanism of the hybrid propellant combustion, low combustion efficiency (≈90%) results from the poor mixing between oxidizer and fuel in the boundary layer over the fuel grain surface when compared to solid rocket system (≈97%).

Compared to the lower combustion efficiency and solid-fuel regression rates, the hybrid rocket propulsion systems have many major advantages over conventional solid- and liquid-propellant rockets, especially in view of safely, higher density impulse, production costs, minimized environmental impact, on/off operational capability, thrust modulation, and greater controllability. Regarding these advantages, it is of great interest to improve solid-fuel technology as well as to explore new advanced energetic fuel ingredients that can be constituents of potential generation of solid fuels.

Due to the mechanism of the propellant combustion, the regression behavior of a hybrid engine grain differs considerably from that of a solid rocket propellant. **Table (2)** presents a comparison of the regression behaviors of solid and hybrid rocket motors.

Table 2 Regression behavior of solid and hybrid rocket motors

	Solid rocket motor	Hybrid rocket motor
Dominating combustion mechanism.	- Chemical kinetics.	- Heat transfer.
Main parameter governing regression.	- Combustion chamber pressure.	- Oxidizer mass flux.
Main parameters governing operating point.	- Combustion chamber pressure. - Clamping (ratio of burning area to port area).	- Oxidizer mass flow rate. - Geometry of solid fuel grain.
Other parameters influencing the regression rate.	- Combustion temperature. - Particle size of oxidizer. - Propellant composition. - Initial grain temperature. - Gas velocity. - Propellant configuration.	- Composition of solid fuel grain. - Melting point. - Flame temperature. - Combustion chamber pressure.

2: OBJECTIVES AND PREVIOUS WORK

The main target of the present article is to make a comprehensive theoretical and experimental analysis on the effect of design parameters and operating phenomena of the HRM. A small scale HRM has been designed, manufactured and tested, with different initial port diameter of fuel grain (5, 20 and 28mm) and different Al powder percent (2.5, 5.0, 7.5, 10.0, 12.5, and 15.0%). The used propellant was PE in the form of a tubular grain as fuel and gas oxygen as oxidizer [20].

The Hybrid propellant selected as a combination of PE, GO2 and Al powder, PE as solid fuel, its good machinability, low cost, acceptable performance, availability, and safe combustion products, GO2 as oxidizer based on quality of handling, storability, transportability, ignition and toxicity. Finally; choice Al powder as energetic material is based on its thermal properties, ease of processing, and relatively low cost.

The experiments took place for chamber pressure up to 15 bar, firing duration about 5 sec, fuel grain length about 75mm, oxidizer mass flow rate up to 14 gm/s.

Ignition by hot air proved to be a very attractive ignition method, for its higher safety, higher reliability and acceptable delay time (less than 1.7 s.).

The re-start operation was demonstrated several times and can be carried out more easily with hot air ignition method.

A mathematical model has been implemented to solve for the regression rate, chamber pressure-time history and other key performance parameters.

The program was validated through the comparison of predicted and measured performance parameters for a small-scale hybrid test motor.

Comprehensive theoretical and experimental investigations on parameters that affect the performance of hybrid motor have been carried out. The effects of mass flux, geometry of the fuel grain and post combustion chamber on performance have been studied. The comparison between test data and computational results show good agreement [20].

3: DESIGN PARAMETERS THEORETICAL STUDY

3.1: Effect of the Fuel Grain Port Geometry

Since the regression surface A_{bu}, and the cross section area A_{po} are both dependent on the active channel radius, the fuel mass flow rate $\dot{m}_{fu}$ will generally change as burning progresses. Both the mixture ratio O/F and the combustion chamber pressure P_c will therefore vary with time.

At steady state operation, the mass conservation implies.

$$\frac{P_c A_{th}}{C^*} = \dot{m}_{ox} + \dot{m}_{fu} \qquad \text{Eq. (1)}$$

The simplified formula for fuel mass flow rate is defined as:

$$\dot{m}_{fu} = a\left(\frac{\dot{m}_{ox}}{A_{po}}\right)^n L_{fu}^m A_{bu} \rho_{fu} \qquad \text{Eq. (2)}$$

$$\frac{P_c A_{th}}{C^*} = \dot{m}_{ox} + a\left(\frac{\dot{m}_{ox}}{A_{po}}\right)^n L_{fu}^m A_{bu} \rho_{fu} \qquad \text{Eq. (3)}$$

where, A_{th} nozzle throat area, C^* characteristic velocity, a regression rate coefficient, n,m regression rate constants, L_{fu} fuel grain length, $\dot{m}_{ox}$ oxidizer mass flow rate and ρ_{fu} fuel grain density.

At fixed $\dot{m}_{ox}$, the changes in the operating point parameters P_c, O/F and C^* are caused by the term $A_{bu} A_{po}^{-n}$, and all other effects must therefore be understood as a consequence of this consideration.

Given a hollow cylinder grain length L_{fu}, the geometric parameters are.

$$\left.\begin{aligned} A_{po} &= \left(\pi/4\right) d_{po}^2 \\ A_{bu} &= \pi d_{po} L_{fu} \end{aligned}\right\} \qquad \text{Eq. (4)}$$

Therefore, $A_{bu} A_{po}^{-n} = \text{constant} d_{po}^{1-2n}$

It follows from this equation that in case of a cylindrical port grain, if no change of the operating point is required, the oxidizer mass flux exponent n should be equal to 0.5.

3.2: Prediction of Port Diameter Variation at Constant Oxidizer Flow Rate

It is nice to be able to predict the actual port diameters at any given instance of time by a simplified equation. Beginning with the fuel regression rate, $\dot{r}_{fu}$ as [18,19]:

$$\dot{r}_{fu} = a G_{ox}^n L_{fu}^m \qquad \text{Eq. (5)}$$

Where, G_{ox} oxidizer mass flux. The change of port diameter d_{po} with operating time t_{bu} can be determined as follows.

$$\dot{r}_{fu} = \frac{1}{2}\frac{d d_{po}}{dt} = a\left(\frac{4\dot{m}_{ox}}{\pi d_{po}^2}\right)^n L_{fu}^m \qquad \text{Eq. (6)}$$

$$\frac{1}{2}\frac{d\,d_{po}}{dt} = a\left(\frac{4\dot{m}_{ox}}{\pi}\right)^{n} L_{fu}^{m}\, d_{po}^{-2n} \qquad \text{Eq. (7)}$$

$$\int_{d_{po,i}}^{d_{po}} d_{po}^{2n}\, d\,d_{po} = 2a\left(\frac{4\dot{m}_{ox}}{\pi}\right)^{n} L_{fu}^{m} \int_{0}^{t} dt \qquad \text{Eq. (8)}$$

Integration leaves a general expression for the instantaneous diameter of the circular port grain as

$$d_{po}(t) = \left[2a(2n+1)\left(\frac{4\dot{m}_{ox}}{\pi}\right)^{n} L_{fu}^{m}\, t + d_{po,i}^{(2n+1)}\right]^{\frac{1}{2n+1}} \qquad \text{Eq. (9)}$$

3.3: Effect of the Fuel Grain Length

Since in the case of HRM, the P_c and therefore also the thrust go under variations during the combustion period, the current dimensions of the solid fuel grain (SFG) can be determined only in relation to a particular point of time in the operating cycle.

Using initial thrust F_i, initial mixture ratio ϕ_I and specific impulse $I_{sp,i}$,one obtains the initial $\dot{m}_{ox}$ as

$$\dot{m}_{ox} = \frac{F_i}{I_{sp,i}\, g\left(1 + 1/\phi_i\right)} \qquad \text{Eq. (10)}$$

Recalling Eq. 2 $\qquad \dot{m}_{fu} = a\, L_{fu}^{m}\left(\frac{\dot{m}_{ox}}{A_{po}}\right)^{n} A_{bu}\rho_{fu}$

The initial geometry parameter can be written as:

$$A_{bu,i}\, A_{P_{o,i}}^{-n} = \frac{1}{\phi_i \rho_{fu}\, a\, L_{fu}^{m}}\left[\frac{F_i}{I_{sp,i}\, g(1+\frac{1}{\phi_i})}\right]^{1-n} = K_o \qquad \text{Eq. (11)}$$

The right hand side of the above equation can be assumed as constant k_o for any design mission. Since burning surface $A_{bu,i}$ is proportional to the length of the propellant grain, this means the thrust increases as the length of the fuel grain raised to the power 1/(1-n) ($F \propto L_{fu}^{1/(1-n)}$).

For n=0.5 then $F \propto L_{fu}^{2}$, therefore, high thrust requirements leads to long fuel grains.

3.4: Prediction of Mixture Ratio Shift

The SFG charge must be designed in accordance with the particular demands of the required mission. The dimensions of the solid fuel should satisfy minimum shift of O/F with operating time while securing maximum hybrid performance.

The main disadvantage of HRM consists in the shifting O/F during the operation; it would be desirable to design a motor that operates at or near the optimum O/F. This value is absolutely different from the stochiometric mixture ratio $(O/F)_{sto}$.

During the firing operation, the A_{po} increases for a fixed $\dot{m}_{ox}$, the actual O/F will increase during the operation. As a result, a flight motor would be designed to begin combustion at an O/F somewhat lower than the optimum value so the efficiency would be increasing over time with a near optimum integrated efficiency achieved.

The initial O/F from the required flow rates.

$$\left(O/F\right)_i = \frac{\dot{m}_{ox,i}}{\dot{m}_{fu,i}} = \frac{\dot{m}_{ox,i}}{\dot{r}_{fu,i}\,\rho_{fu}\,A_{bu,i}} \qquad \text{Eq. (12)}$$

The final O/F

$$\left(O/F\right)_f = \frac{\dot{m}_{ox,f}}{\dot{m}_{fu,f}} = \frac{\dot{m}_{ox,f}}{\dot{r}_{fu,f}\,\rho_{fu}\,A_{bu,f}} \qquad \text{Eq. (13)}$$

The $\dot{m}_{ox}$ is assumed constant along system operation, then together with Eq. 12 and Eq. 13, the O/F shift can be described as function of change of fuel grain port diameter as:

$$\frac{(O/F)_f}{(O/F)_i} = \left[\frac{d_{po,i}}{d_{po,f}}\right]^{2n-1} \qquad \text{Eq. (14)}$$

The above relation is valid only for tubular grain shape. It can be seen that for n > 0.5, the port area increases during operation and the O/F increases. Notice that at n=0.5, O/F does not vary with change of fuel grain port diameter or operation time.

4: EXPERIMENTAL STUDY

4.1: Effect of Fuel Grain Port Diameter

A series of experimental test motor has been fired for different initial port diameters (5, 20 and 28 mm) with constant fuel grain length (70 to 80 mm) for burning durations around 5 sec. and Al powder weight percentage additives (2.5, 5.0, 7.5, 10.0, 12.5, and 15.0%). As shown in **Figure (2)**, observations of the SFG active channels before and after a burning reveal that, the remaining fuel grain port surface is relatively smooth. Combustion of PE material produces carbon particles in the flame zone that can spread out black carbon to the surface along combustion port. Slight inflating toward the GO2 injection head is also observed, in particular with small initial port 5mm.

The reasons of the ablation in the immediate vicinity of the injection head may be explained by the oxidizer jet injection, which actually strikes the fuel grain, and then the solid material will be deeply eroded at these points of the combustion channel.

The small fuel grain port makes many problems especially after firing with heat exchanger ignition method. The molten PE at the end face of fuel grain moves back to oxidizer injection head and blocks the injectors, **Figure (3)**. These problems could be solved by placing a gasket from insulation material (ASBESTOS) between fuel grain end face and injection head.

On other hand, for fuel grain with small port, neither pyrotechnic charge, nor heat wire, nor fuse wire was able to successfully ignite the fuel grain. High oxygen mass flux invokes coughing ignition spot (initiation point) before built up. Fortunately, hot air ignition method gives excellent ignition results with the small port area.
More smooth fuel grain surface and less soot have been observed when using Al additive. In conclusion, the initial fuel grain port diameter (active channel port) is shown to be one of the critical parameters encountered in HRM design.
Figures (4) and (5) illustrate the effect of initial port diameter (5 mm to 28 mm) on HRM regression rate and average chamber pressure at nearly constant $\dot{m}_{ox}$, and L_{fu} for a variety of Al powder additives (2.5 up to 15% by weight).

Fig. (2) PE Active Channel Port Before and After Firing


Fig. (3) Molten Fuel Material Moves Back to Block Injectors

As seen from **Figure (4)**, the average regression rate decreases with the increase of port diameter. This increase is more significant at lower initial port diameters.
Considering the port diameters from 5.mm to less than 20 mm, it could be seen that the average regression rate increases with increasing the percentage of Al powder up to 7.5%. With the percentage of Al powder higher than 7.5%, the phenomenon is reversed, i.e., the average regression rate decreases with the increase of Al powder up to 15%. This effect is insignificant at 20 mm initial diameter up to 28 mm.
This may be explained by the balance between the effects of Al percentage and the port diameter on the degree of erosion rate of the fuel material.

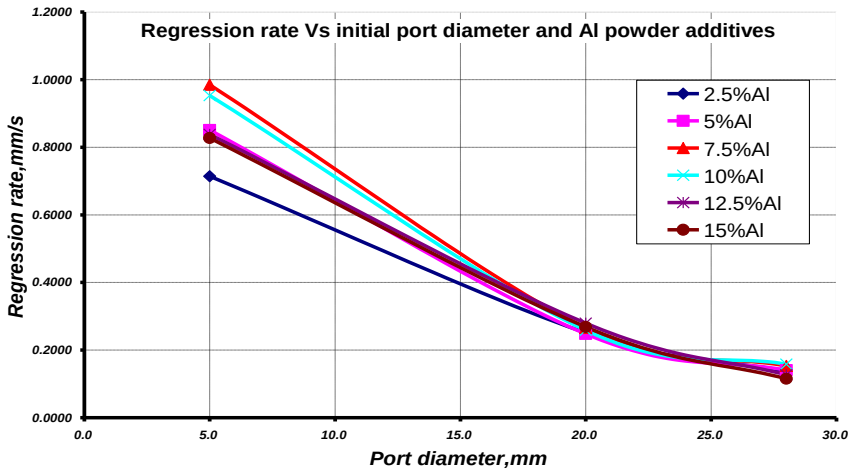

Fig. (4) Regression Rate Versus Initial Port Diameter and Al Powder Additives

Figure (5) describes the variation of average chamber pressure with fuel grain initial port diameter at different Al powder additives.

For initial port diameter 5 mm up to 20 mm, the average chamber pressure slightly decreases with the increase of port diameter. That effect is steeper for port diameters from 20 mm up to 28 mm.

For Al powder from 2.5% up to 7.5%, the average chamber pressure increases with the increase of Al percentage. For Al powder more than 7.5% up to 15% the behavior is reversed, i.e., as the Al% increases the average chamber pressure decreases.

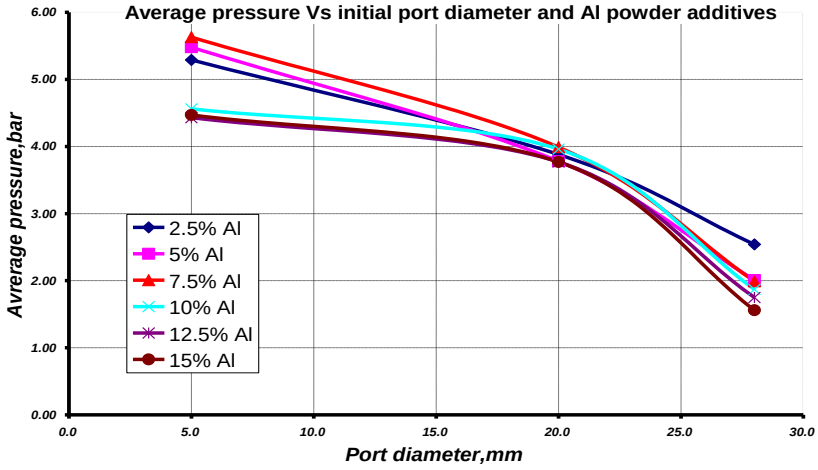

Fig. (5) Average Pressure Versus Initial Port Diameter and Al Powder Additives

Finally, it could be concluded that the addition of 7.5% Al powder gives the highest performance for the case under study. Comparing this case (7.5% Al) with the base line configuration (0% Al) a regression rate increase of 90% and chamber pressure increase of 40% were reached. This has an excellent impact on the overall performance of the HRM with Al additive. It is claimed that it is always possible to deduce the proper Al percentage that leads to the best performance for a given case under study.

For smaller values of initial port diameter of fuel grain, the chamber pressure and regression rate are generally increased.

To compensate the effect of port diameter variation during firing, three solutions are proposed:

- By a special design of fuel grain configuration.
- Using layers of fuel grain with different materials.
- By controlling the oxidizer mass flow rate during the burning time, such that a nearly constant regression rate would be obtained.

4.2: Effect of Oxidizer Mass Flow Rate

The effect of changing the oxidizer mass flow rates on the HRM parameters is summarized in **Table (4)**. The motor dimensions and the propellant characteristics are kept unchanged. It could be shown that, for the range of oxidizer mass flow in these tests, the combustion efficiency decreases as the oxidizer mass flow rate increases. It is believed that, for each specified case, it is possible to find the oxidizer flow rate for which the efficiency would be maximized.

Table (4) shows also that the hybrid motor combustion chamber pressure is strongly dependent on the oxidizer mass flow rate. **Figure (6)** shows the combustion chamber pressure for two different oxidizer mass flow rates.

Table (3)Hybrid Parameters at Different Oxidizer Mass Flow Rates

Parameters	D_{po}=5mm,L_{fu}=80mm,duration ≈5 sec		
	(Test 3/5*)5%Al, $\dot{m}_{ox}$ = 8.7 gm/s	(Test 1/5*)5%Al $\dot{m}_{ox}$ = 9.1gm/s	(Test 2/5*)5%Al $\dot{m}_{ox}$ = 9.2gm/s
Regression rate, (mm/s)	1.0809	0.8509	0.8878
Chamber pressure, (bar)	5.93	5.48	5.44
Mixture ratio, (-)	3.46	4.57	4.08
Experimental C* (m/s)	1495.2	1396.9	1342.5
Theoretical C* (m/s)	1651.4	1588.7	1620.6
Combustion efficiency, (%)	90.5	87.9	82.8

* Details of tests are given in reference [20]

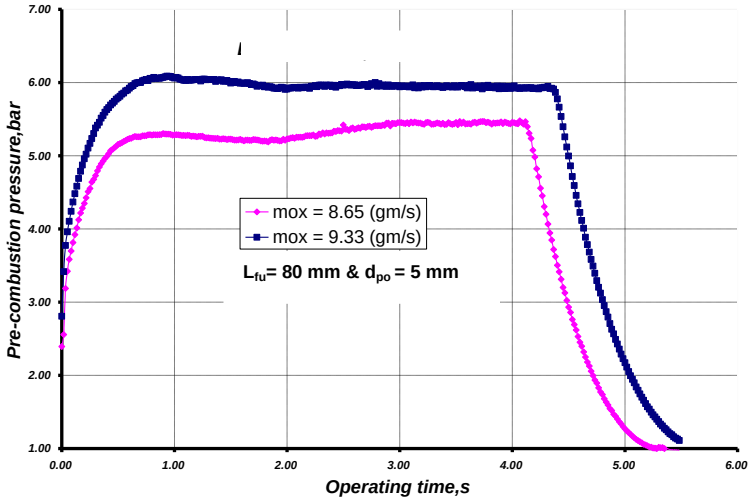

Fig. (6) Combustion Chamber Pressure versus Firing Time

4.3: Effect of Al Powder Additives

The low performance resulting from the poor mixing between oxidizer and fuel in the turbulent boundary layer over the fuel grain surface was recognized in many classical HRM. To overcome this drawback of the conventional HRM, energetic additives were proposed to be used with fuel grain to enhance performance in particular the regression rate and chamber pressure.

Table (4) and **Figure (7)** describe the effect of Al% on the HRM performance, especially chamber pressure, regression rate and combustion efficiency.

Each of the regression rate and chamber pressure increases with the increase of additive Al% to fuel grain material up to 7.5%. With Al% higher than 7.5% poorer combustion efficiency is encountered.

Analysis of experimental results may lead to the following remarks:

1) Ignition delay time decreases with increasing of Al%.
2) Each of the regression rate, the chamber temperature and the chamber pressure increases as Al% increases.

3) The combustion efficiency reaches highest value at 2.5% Al%.
4) No significant variation on the regression rate or performance is observed when using Al powder more 7.5%.

The variation of average experimental regression rates with oxidizer mass flux at different. Al% additives is shown in **Figure (8)**. The regression rate increases more sharply at lower oxidizer mass flux, but the increase gets more flat at higher oxidizer mass flux.

Table (4) Effects of Al Powder Additives

Parameter	Test 1/3* (Base line) (pure PE)	Test 2/4* (2.5%Al)	Test 2/5* (5 %Al)	Test 2/6* (7.5 %Al)
Chamber pressure(bar)	3.92	5.29	5.44	5.63
Average mixing ratio(-)	6.91	6.62	9.2	8.9
Regression rate(mm/s).	0.5146	0.7143	0.8878	0.9848
Experimental C* (m/s).	913.5	1397.3	1342.5	1368.5
Theoretical C* (m/s).	1479.8	1490.8	1620.6	1676.7
Combustion efficiency (%).	61.7	93.7	82.8	81.6

* Details of tests are given in Reference [20]

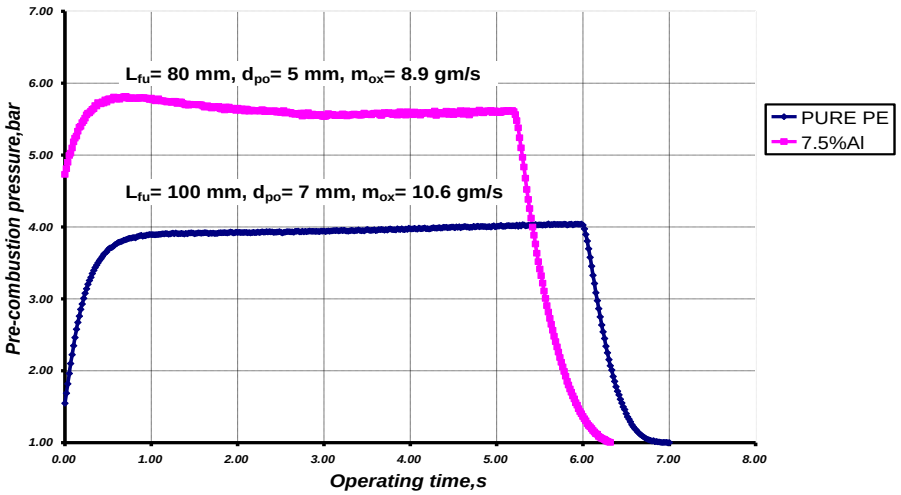

Fig. (7) Chamber Pressure Versus Time, with and Without Al Powder

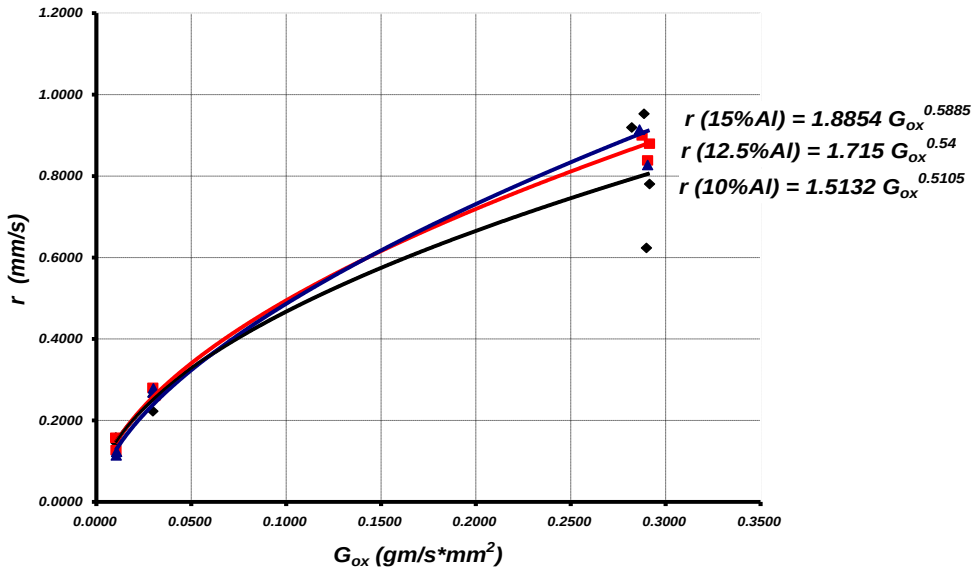

Fig. (8) Regression Rates with Various Oxidizer Mass Fluxes at Different Al%

4.3.1: Formulation of the Regression Rate

Making use of the experimental data now available, it is worthy to express the regression rate as function of mass flux with consideration of Al% addition. The data are plotted in **Figure (9)** and two representative curves that describe the trends of variation are traced. These trends are mathematically expressed to reflect the empirical regression rate as follows:

For $Al \leq 7.5\%$ $\quad \dot{r} = 2.0357 G_{ox}^{0.5688}$ (mm, gm, s) Eq. (15)

For $Al > 7.5\%$ $\quad \dot{r} = 1.6657 G_{ox}^{0.5417}$ (mm, gm, s) Eq. (16)

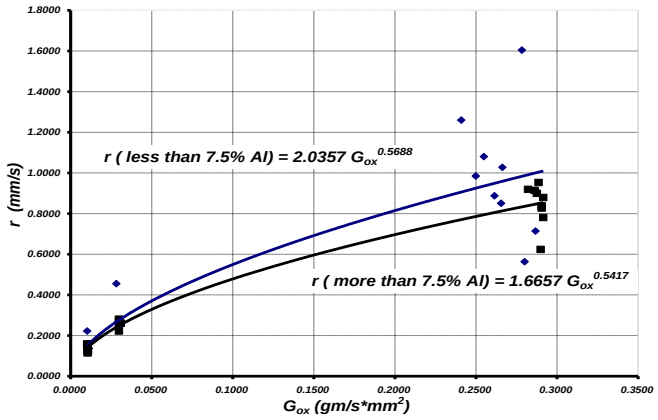

Fig. (9) Al Powder % Effect Regime on the Regression Rate

4.3.2: Effect of Al Particles on Nozzle Throat

One of the problems encountered is that a quite large amount of solid aluminum particles is formed during the expansion (exhaust gases). These solid particles cause erosion of nozzle throat, especially at high oxidizer mass flux or long duration. Enlargement of the nozzle throat dimensions is the direct consequence of the effect of Al particles, **Figure (10)**. The thrust magnitude will be changed accordingly, but a pre-knowledge of such behavior would help compensate this effect.

Fig.(10) Nozzle Throat as Affected by Al Particles

5: PHENOMENA STUDY

5.1: Throttling Operation

Thrust modulation could be achieved either through a change of the throat area or the combustion pressure. Nozzle throat variation is extremely difficult during operation. So, thrust modulation through pressure variation can be used. Pressure change may be realized by controlling the main flow rate of oxidizer injection.

The thrust of HRM could be regulated and terminated using a single controlling valve at oxidizer feeding line (solenoid valve normally closed).Increasing the oxidizer mass flow results in an increasing mixture ratio O/F value and a part of propellant remains un-reacted in the combustion chamber. Another important problem associated with throttling is the increasing instability of combustion, due to change in feeding system characteristics.

Figure (11) shows a record of throttling in the supply line of oxidizer gas. The variation of pressure and temperature is represented by two pulses that describe the transition caused by closing and opening the valve in the gas line.

From the figure, it can be seen that values of chamber pressures are varied depending on the variations in the oxidizer flow rate. A throttling capability (maximum to minimum chamber pressure) of (10.7/4.1) could be achieved by the decreasing oxidizer flow rate by 14.4 % (10.4 to 8.9 gm/s).

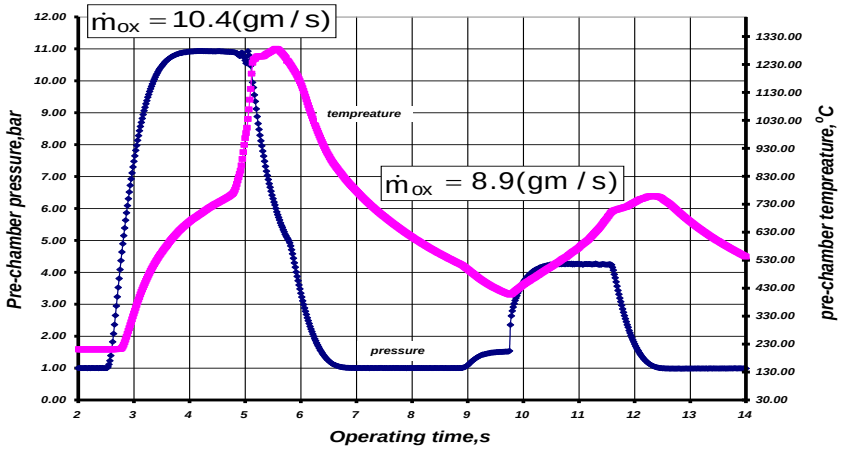

Fig. (11) Throttling Operation of Hybrid Rocket Motor

5.2: Exhaust Flame (Plume) Properties

The visualization results of practical HRM are obtained for PE with Al powder as fuel plus gaseous oxygen as oxidizer. **Figure (12)** shows a direct photograph during steady combustion at 3 sec after ignition, the plume, which is constructed under an atmospheric pressure, is formed at the immediate vicinity of exit nozzle. Observing the plume gives evidence that combustion is still occurring along the combustion gases after leaving the nozzle. The exhaust gases contains high amount of unburned fuel and several particles of Al powder which react with atmospheric oxygen. This is demonstrated by the red color observed around the plume, which means lower combustion efficiency of HRM.

The exhaust plume configuration changes according to nozzle shape, **Figure (13) Table (5)** describes the distribution of exhaust gas temperature along the plume length for different Al% additives. These results were calculated using thermo chemical calculations [21].

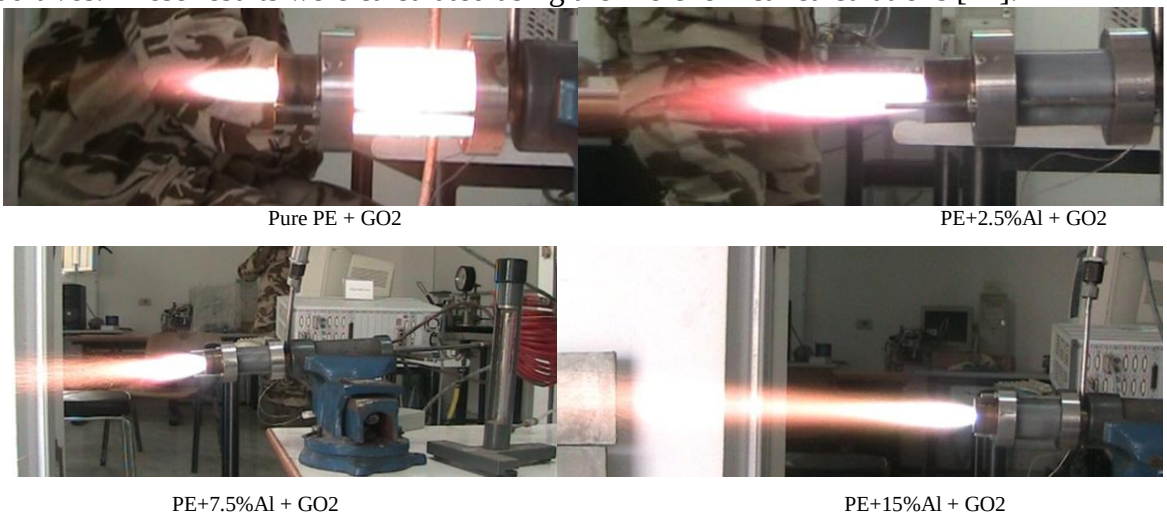

Pure PE + GO2 PE+2.5%Al + GO2

PE+7.5%Al + GO2 PE+15%Al + GO2

Fig. (12) Exhaust Plume Jet during Combustion

d_{th}=3 mm with area ratio = 10, P_C = 2.01bar d_{th}=5 mm with area ratio = 15, P_C = 4.47 bar

Fig. (13) Exhaust Flame (Plume) Shape for Different Nozzle Shape

Table (4) Theoretical Exhaust Flame Plume Temperature (K)
forPE, AlAdditives with GO_2at P_c=7bar, O/F=2

Plume length	**Exhaust flame plume temperature (k)**						
	pure	**2.5%Al**	**5%Al**	**7.5%Al**	**10%Al**	**12.5%Al**	**15%Al**
ε= 1	2999.85	3053.93	3105.80	3152.59	3195.10	3234.80	3270.09
ε=adapted nozzle	2497.64	2581.93	2658.90	2728.39	2790.43	2845.32	2893.89
ε= 10	1634.47	1750.17	1872.44	1998.87	2124.96	2244.75	2326.99
ε= 15	1470.64	1578.75	1695.01	1819.04	1948.25	2077.84	2200.40
ε= 20	1365.92	1468.04	1578.88	1698.63	1826.19	1958.29	2088.67

6:. CONCLUSION

A small scale HRM has been designed, manufactured and tested by using different initial port diameter and length of PE fuel, different metalized Al powder percent as fuel additives and GO2 as oxidizer.

The first phase of the study is devoted to study the effect of design parameters theoretically. Results can be summarized as follows:

- At fixed oxidizer mass flow rate, the changes in the operating point parameters P_c, O/F and C^* are caused by the term $A_{bu}A_{po}^{-n}$, and for tubular fuel grain, $A_{bu}A_{po}^{-n} = \text{constant} d_{po}^{1-2n}$, if no change of the operating point is required, the oxidizer mass flow flux exponent n should be is equal to 0.5.

- It is nice to be able to predict the actual fuel port diameters and O/F shift at any given instance of firing time.
- For regression rate, mass flux constant n > 0.5 the port area increases during operation and the O/F increases during firing. Notice that at n=0.5, O/F does not vary with change of fuel grain port diameter or operation time.
- Since burning surface $A_{bu,i}$ is proportional to the length of the fuel grain, this means the thrust increases as the length of the fuel grain raised to the power 1/(1-n), For n=0.5 then $F \propto L_{fu}^{2}$, therefore, high thrust requirements leads to long fuel grains.

During the second phase of the study, the experimental work has lead to the following conclusions:

- Observations of the fuel grain active channels before and after firings reveals that, the remaining fuel port surface is relatively smooth with black carbon traces and slight inflating near the injection head. This is better demonstrated with small initial port (5mm).
- Regression rate of hybrid fuel grain was enhanced by addition of Al powder. Adding up to 7.5% gives the best performance as regression rate increases by 90% and chamber pressure increases by 40% compared to basic configuration (0% Al).
- Adding Al powder to PE fuel proved to have the following impact on performance
  - More smooth fuel grain surface and less soot have been observed when using Al.
  - Higher regression rates are more significant at Al powder additive increased up to 7.5% by mass.
  - Combustion efficiency reaches about 93% with addition of 2.5%Al%.
  - Less instability is achieved as compared with pure PE combustion.
  - Metal additives lead to decreased nozzle life due to high temperature and erosive effect.
  - Reduced emissions of product gases (soot, unburned hydrocarbons).

A throttling capability (maximum to minimum chamber pressure) of (10.7/4.1) could be achieved by the oxidizer flow rate changed by 14.4 % decreases (10.4 to 8.9 gm/sec) during experimental work.

7: REFERENCES

[1] David, A., “Hybrid Rocket Development History,” AIAA-No. 91-2515, June 24–26, 1991.

[2] Loh, W.H.T., “Jet, Rocket, Nuclear, Ion, And Electric Propulsion: Theory And Design,” New York: Springer-Verlag, 1968.

[3] Lengelle, G., "Hybrid Propulsion, Historical Aspect. Context. International Activities," Energetic Dept., ONERA, France, Jan. 2003

[4] Winfried M.S., and Schmucker, R.H., “Development of A Small Hybrid Rocket Motor,” Institute of astronauts, Technical University Munchen, Sep. 1971.

[5] Winfried M.S., and Schmucker, R.H., “Influence of Different Parameters on the Starting Behavior Of Hybrid Engines,” Institute of Astronauts, Technical University Munchen, 14 April, 1974.

[6] Tuzinsk, W.A., “Hybrid Rocket,” Institute of Astronauts, Technical University Munchen, 14 April 1970.

[7] Gany, A., Timnat, Y.M., and Wolfshtein, M., “Tow-Phase flow Effects on hybrid Combustion,” ActaAstronautica, Vol. 3, PP. 241-263, 1976.

[8] Gany, A., and Timnat, Y.T., “Parametric Study Of a Hybrid Rocket Motor,” Israel Journal of Technology, Vol. 10, No. 1-2, PP. 85-96, 1972.

[9] Gany, A., “Scale Effects in Hybrid Motor Under Similarity Conditions,” AIAA 96-2846, July 1996.

[10] Paul, P.J., Jain, V.K., and Chanda, M., “Studies on the Hybrid Rocket Motor,” Proc. Indian Acad. Sci., Vol. C2, part 1, May 1979, PP. 525-533.

[11] Hukunda, H.S., Jain, V.K., and Paul, P.J., “A Review of Hybrid Rockets: Present Status and Future Potential,” Proc. Indian Acad. Sci., Vol. C2, part 1, May 1979, PP. 215-242.

[12] Lydon, M.C., and Simmons, R.J., "Hybrid Sounding Rocket Development at the United State Force Academy,"
[13] Greiner, B., and Frederick, R.A., "Results of Lab-scale Hybrid Rocket Motor Investigation," AIAA 92-3301, July 1992.
[14] Wolfhard, H.G., Glassman, L., and Leon G., "Heterogeneous Combustion," Technical Papers Based on AIAA, Academic Press, New York, 1964
[15] Sellers, J.J., "Investigation into Low-Cost Propulsion Systems for Small Satellite Missions," Ph.D. Thesis, University of Surrey, June 1996
[16] Brown, R and Seller, J.J., "Practical Experience with Hybrid Peroxide Hybrid Rocket," 1st Hydrogen Peroxide Workshop, Guilford, Surrey, 1998.
[17] Murthy, K.M., and Jain, S.R., "Studies on Some Novel Hypergolic Hybrid Systems," IAF 87-271, October 10–17, Brighton, UK, 1987.
[18] Humble, R., Henry, Gary, N.and Larson, Wiley, J., "Propulsion System Analysis and Design," United States Air Force Academy, 1995.
[19] Sutton, G., "Rocket Propulsion Elements," Sixth Edition, John Wiley, New York, 1992.
[20] Capt. Eng. Meteb K. J. Al-Timimi, "Prediction of Hybrid Rocket Motor Regression Rate"M.Sc thesis, MTC, Cairo, Aug. 2009.
Selph, C., "Computer Program For Calculation of Complex Chemical Equilibrium Composition," NASA SP-273, United States Air Foece Academy, version, July 1994.